

WISE DETECTION OF THE GALACTIC LOW-MASS X-RAY BINARIES

XUEBING WANG¹ AND ZHONGXIANG WANGKey Laboratory for Research in Galaxies and Cosmology, Shanghai Astronomical Observatory,
Chinese Academy of Sciences, 80 Nandan Road, Shanghai 200030, China*Draft version August 20, 2019*

ABSTRACT

We report on the results from our search for the Wide-field Infrared Survey Explorer detection of the Galactic low-mass X-ray binaries. Among 187 binaries catalogued in Liu et al. (2007), we find 13 counterparts and two candidate counterparts. For the 13 counterparts, two (4U 0614+091 and GX 339–4) have already been confirmed by previous studies to have a jet and one (GRS 1915+105) to have a candidate circumbinary disk, from which the detected infrared emission arose. Having collected the broad-band optical and near-infrared data in literature and constructed flux density spectra for the other 10 binaries, we identify that three (A0620–00, XTE J1118+480, and GX 1+4) are candidate circumbinary disk systems, four (Cen X-4, 4U 1700+24, 3A 1954+319, and Cyg X-2) had thermal emission from their companion stars, and three (Sco X-1, Her X-1, and Swift J1753.5–0127) are peculiar systems with the origin of their infrared emission rather uncertain. We discuss the results and WISE counterparts' brightness distribution among the known LMXBs, and suggest that more than half of the LMXBs would have a jet, a circumbinary disk, or the both.

Subject headings: binaries: close — infrared: stars — stars: black holes — stars: low-mass — stars: neutron

1. INTRODUCTION

X-ray binaries (XRBs), containing either an accreting neutron star or black hole, constitute a large fraction of bright X-ray sources in the Galaxy. When they have $\lesssim 1 M_{\odot}$ low mass companions, a companion overfills its Roche lobe, and mass transfer from the companion to the central compact star occurs via an accretion disk. Such binaries are further categorized as low-mass X-ray binaries (LMXBs). Besides their prominent X-ray emission, LMXBs are generally observable at optical wavelengths, as the accretion disks and/or companion stars radiate sufficiently bright thermal emission. In addition, the LMXBs are known to be able to launch a jet, producing synchrotron emission detectable from optical/infrared to radio wavelengths (e.g., Fender 2006; Russell et al. 2006, 2007; Gallo 2010). Studies of jets help understand flux variabilities seen in LMXBs, constrain the fractions of accretion energy channeled to different emission components, and thus allow to draw a full picture for the detailed physical processes occurring in LMXBs.

The environments in which XRBs are located may be dusty. The supernova explosions that produced the compact stars are thought to have a fallback process (Chevalier 1989), due to the impact of the reverse shock wave with the outer stellar envelope. As a result, part of the ejected material during a supernova explosion may fallback to the newly born compact star. During the evolution of a LMXB, a substantial amount of mass has been lost from the companion (e.g., Podsiadlowski et al. 2002). Observational evidence as well as theoretical studies show that disk winds or outflows are probably ubiquitous and may be massive (e.g., Neilsen 2013; Yuan et al. 2012 and references therein). If a small fraction of the material from any of the processes is captured to be

around a binary, it is conceivable that a circumbinary disk might have formed from the material, acting to intercept part of emission (X-rays from the central compact star and optical light from the companion and accretion disk) from the binary system and re-radiate the energy at infrared (IR) wavelengths. Indeed, Munro & Mauerhan (2006) observed four LMXBs with *Spitzer* Space Telescope and found that two of them might harbor a circumbinary dust disk. Moreover, the *Spitzer* detection of dust emission features in a so-called microquasar (see, e.g., Gallo 2010) clearly indicates the existence of dust material around the LMXB (Rahoui et al. 2010).

The Wide-field Infrared Survey Explorer (WISE), launched in 2009 December, mapped the whole sky at its bands of 3.4, 4.6, 12, and 22 μm (called W1, W2, W3, and W4, respectively) in 2010 (Wright et al. 2010). The FWHMs of the averaged point spread function for WISE imaging at the four bands were 6''.1, 6''.4, 6''.5, and 12''.0, and the sensitivities (5σ) generally reached were 0.08, 0.11, 1, and 6 mJy. In the WISE all-sky images and source catalogue released in 2012 March, measurements of over 563 million objects are provided. Therefore WISE imaging has provided sensitive measurements of many different types of celestial objects at the IR wavelengths (see Wright et al. 2010 for details).

Using the WISE data, we have carried out searches for the counterparts to the LMXBs catalogued in Liu et al. (2007), for the purpose of identifying sources among them with either jets or circumbinary debris disks. In this paper we report the results from our searches.

2. DATA ANALYSIS

The LMXB catalogue contains 187 sources in the Galaxy, Large and Small Magellanic Cloud (Liu et al. 2007). The general properties of these sources, for example their coordinates, magnitudes in the *UBV* bands, estimates of the interstellar reddening $E(B - V)$, X-ray

¹ Graduate University of Chinese Academy of Sciences, No. 19A, Yuquan Road, Beijing 100049, China

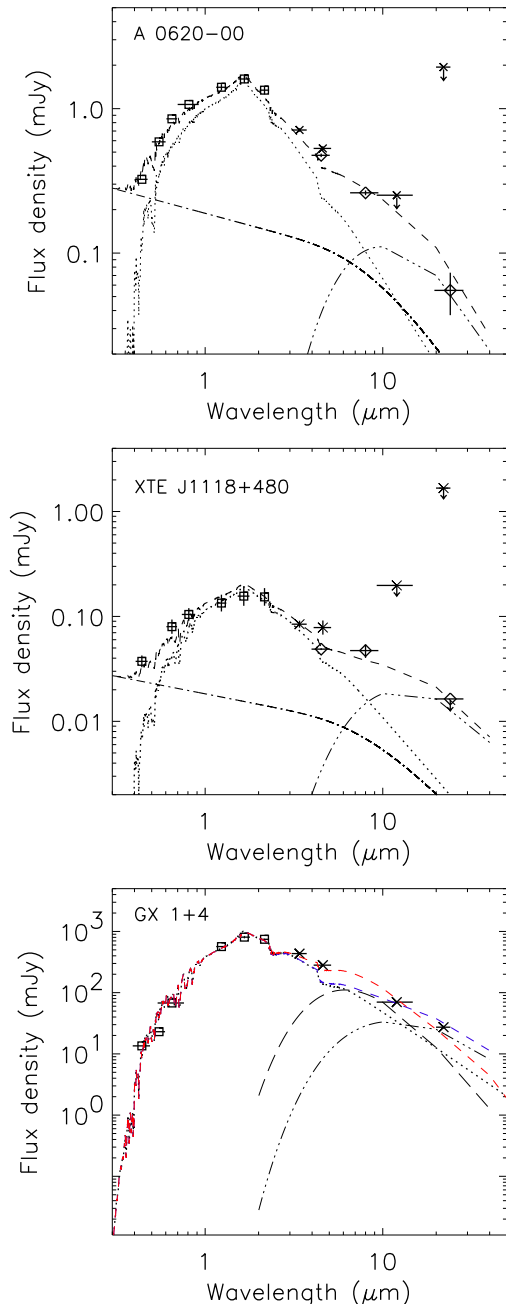


FIG. 1.— Flux density spectra of A0620–00, XTE J1118+480, and GX 1+4. The squares and diamonds are optical/near-IR and *Spitzer* data points, respectively, and crosses are the WISE data points. The dotted, dash-dotted, and dash-triple-dotted curves represent emission from the companions, accretion disks, and circumbinary disks, respectively. The dashed curves (blue one for GX 1+4) represent the total emission from all the components. For GX 1+4, the long dashed curve represents emission from a dust shell, and a red dashed curve is the total emission from the companion and the dust shell.

types, are provided when such information is available in literatures. The X-ray types such as X-ray burst source, X-ray pulsar, or microquasar, allow to know whether the primary compact object is a black hole or a neutron star.

We input the coordinates of the LMXBs given in the catalogue into WISE Source Catalog query, provided at the NASA/IPAC Infrared Science Archive. Given the FWHMs of WISE imaging, we used a $2''.0$ radius (see

Debes et al. 2011 for details) around the coordinates for counterpart searching. All sources located in globular clusters were excluded because of the high density of stars in a cluster. Candidate counterparts to 17 LMXBs were found. For them, we further checked the uncertainties for their reported source positions, and found that most of them have positional uncertainties of $\lesssim 1''$, sufficiently small comparing to the $2''$ search radius. However among them, the position of 4U 1735–28 has an uncertainty of $7'$ (Forman et al. 1978), too large for finding the counterpart, and it was excluded. In addition for SLX 1737–282, the position in the LMXB catalogue was from in't Zand et al. (2002), which has an uncertainty of $8''.3$. A *Chandra* position was reported by Tomsick et al. (2008), which has an uncertainty of $0''.6$ and an offset of $3''.3$ from the WISE source. The WISE source was detected by 2MASS (Skrutskie et al. 2006) at *JHK_s* bands, which was already excluded as the counterpart to SLX 1737–282 by Tomsick et al. (2008). Further checking the previous optical/IR studies of each of the sources, we concluded that counterparts to 13 LMXBs and candidate counterparts to 2 LMXBs were found. The offsets of the WISE source coordinates from the input ones of the 15 LMXBs are summarized in Table 1. The WISE magnitude measurements or upper limits of them, as well as 2MASS *JHK_s* measurements if they were detected, are also given in Table 1.

To determine any excess emission in the IR bands, thermal emission from a companion star has to be often considered. On the basis of the reported spectral types for the companion stars, we used stellar atmosphere models of the Kurucz (1993) to estimate the thermal emission. If any flux measurements at optical and near-IR bands for a source are available, the information was collected and then used to construct a broad-band spectrum, which is required for the determination of the presence of any excess emission. The reddening values to the LMXBs were also collected in order to deredden the observed fluxes. The reddening laws of Schlegel, Finkbeiner, & Davis (1998) for the optical and near-IR data, and Indebetouw et al. (2005) (wavelengths $\leq 8 \mu\text{m}$) and Weingartner & Draine (2001) (wavelengths $> 8 \mu\text{m}$) for *Spitzer* (when included) and WISE data were used. The information of the binary types, orbital periods, distance estimates from observations, optical photometric bands, and reddening values for the 15 LMXBs, which was used for the construction and analysis of broad-band spectra, is summarized in Table 2.

3. RESULTS

3.1. Candidate circumbinary debris disk systems

On the basis of their broad-band spectra and previous multi-wavelength studies, we identified four LMXBs with a candidate circumbinary debris disk. They are A0620–00, XTE J1118+480, GX 1+4, and GRS 1915+105. For the last source, while it is a well-known X-ray binary with a jet (Fender & Belloni 2004), multiple *Spitzer* mid-IR spectroscopic observations have detected PAH features in its emission, clearly indicating the existence of (possibly) a circumbinary dust disk (Rahoui et al. 2010). Comparing the *Spitzer* flux measurements given by Rahoui et al. (2010) with that from WISE, the flux values are comparable given the source

is highly variable. We refer to Rahoui et al. (2010) for detailed models built to explain the mid-IR emission.

For A0620–00 and XTE J1118+480, targeted *Spitzer* imaging was carried out and the detection and identification of circumbinary disks was reported by Munro & Mauerhan (2006). In Figure 1, their dereddened broad-band optical and IR flux density spectra are shown, and the *Spitzer* flux measurements or upper limit are included (diamonds in Figure 1). As can be seen, the WISE measurements or upper limits are generally consistent with the *Spitzer* data (note that for faint, $\gtrsim 14$ mag sources, WISE measurements have large uncertainties and biases², which may be the cause for a brighter W2 flux detected from XTE J1118+480 than that at *Spitzer* 4.5 μ m band).

For A0620–00 and XTE J1118+480, we re-studied their debris disks with updated information and optical and near-IR data. Using the spectral types, estimated distances, and binary parameters published in literatures (see Table 2), a stellar spectrum plus that of a standard optically thick, geometrically thin accretion disk (Shakura & Sunyaev 1973; Frank, King, & Raine 2002) were combined to describe the observed optical and near-IR flux densities. For A0620–00, the masses of the black hole primary and companion and thus the binary orbit’s inclination angle i used were 11 and 0.7 M_{\odot} , and 41° (Gelino et al. 2001), respectively. For XTE J1118+480, they were 8.5 and 0.4 M_{\odot} , and 68° (Gelino et al. 2006). For the black hole systems in quiescence, the inner edge of a standard accretion disk is not certain (e.g., Yuan & Narayan 2014), but the uncertainty affects very little of optical fluxes considered here. The outer edge of a disk was set at 90% of the Roche lobe radius of a primary, at which the disk should be tidally truncated (Frank et al. 2002). The only free parameter adjusted to describe the optical and near-IR data was the mass accretion rate \dot{M} in the disk. We found that $\dot{M} \simeq 1.5 \times 10^{14}$ g s^{−1} and 5.5×10^{13} g s^{−1} for A0620–00 and XTE J1118+480, respectively, were required to produce the model spectra displayed in Figure 1. The values are approximately consistent with those reported in Munro & Mauerhan (2006).

In order to fully describe the overall broad-band spectrum of either A0620–00 or XTE J1118+480, a third component is apparently needed for the excess IR emission seen in the both systems. Arguments for supporting the existence of a circumbinary disk were discussed by Munro & Mauerhan (2006). Here following their work, the same disk model, $T_{\text{disk}} \sim T_* r^{-3/4}$ where T_{disk} is the disk temperature at radius r and T_* is the temperature of a companion, was used to fit the excess emission. The inner disk radius from the center of masses of a binary was set to be $1.7a$ (Taam, Sandquist, & Dubus 2003; Munro & Mauerhan 2006), where a is the binary separation. To simplify the model, the inclination angle of the disk was set to be aligned with that of the orbit, and the only free parameter was the outer disk radius r_o . We found that $r_o = 2.3a$ and $4.5a$ for A0620–00 and XTE J1118+480, respectively, were required to fit the excess emission (see Figure 1).

Having an orbital period of 1160.8 days, the identi-

fied M6III companion in GX 1+4 can not fill its Roche lobe (Hinkle et al. 2006 and references therein). This explains the lack of emission from an accretion disk in its broad-band optical and near-IR spectrum. However the WISE fluxes clearly indicate the excess emission from the source. Using the model above, in which the neutron star primary and companion masses of 1.35 and 1.0 M_{\odot} , respectively, and $i \simeq 70^{\circ}$ were assumed (Hinkle et al. 2006), a circumbinary disk with an outer radius of $2a$ can provide an acceptable fit to the excess emission although the model fluxes (blue dashed curve in Figure 1) at W1 and W2 bands are slightly lower than the observed. A smaller than $1.7a$ inner disk radius is required in order to eliminate the deviation. Since a mass-ejecting outflow is expected from a giant star and optical spectroscopy has suggested the presence of a 6×10^{13} cm radius gas envelope around the binary (Davidsen et al. 1977), we also tested to fit the excess emission with a model of an optically thin dust shell (Waters, Cote, & Geballe 1988; see also van der Veen et al. 1994). We simplified the model by assuming the temperature of 1200 K at the inner edge of the dust shell (the dust sublimation temperature), the emission efficiency of dust grains $Q(\nu) \sim \nu^2$, the number density distribution of the dust shell $n(r) \sim r^{-2}$, where r is the radius, and thus temperature function $T(r) \sim r^{-1/3}$. The model emission from such a dust shell is displayed in Figure 1, and it provides an acceptable description to the excess emission too and is able to eliminate the deviation at W1 and W2 bands when the circumbinary disk model was considered. The total number of dust grains in the shell is $\simeq 1.8 \times 10^{37}$, resulting in a mass of $10^{-10} M_{\odot}$ when assuming 3 g cm^{−3} for the density of grain material (grain radius of 0.1 μ m was assumed). The mass value is a reasonable estimate for the dust around a giant star.

3.2. Jet systems

The neutron star LMXB 4U 0614+091 was detected by WISE at its first three bands. This binary has been well studied from previous targeted *Spitzer* observations and its IR emission has been identified to be from a jet (Migliari et al. 2006, 2010). The WISE fluxes at W1, W2, and W3 were 0.13 ± 0.01 , 0.15 ± 0.02 , and 0.61 ± 0.14 mJy, respectively. Given that the source was faint to WISE, we consider the WISE measurements are consistent with that of *Spitzer* (e.g., Migliari et al. 2010), although flux variability is also expected for a jet. Since detailed, simultaneous multi-band studies of the binary and its jet emission have been presented by Migliari et al. (2010), no further data analysis was conducted for the source.

The black hole binary GX 339–4 has long been known to have a jet (e.g., Corbel & Fender 2002 and references therein). Combining with quasi-simultaneous data of a large wavelength range from radio to X-ray, Gandhi et al. (2011) have already analyzed the WISE data for the binary in detail and showed that the WISE band emission was from a jet of the binary system.

3.3. Companion stars

On the basis of their broad-band spectra, the companion stars in the LMXBs Cen X-4, 4U 1700+24, 3A 1954+319, and Cyg X-2 were identified to have been de-

² see http://wise2.ipac.caltech.edu/docs/release/allsky/expsup/sec6_3c.html

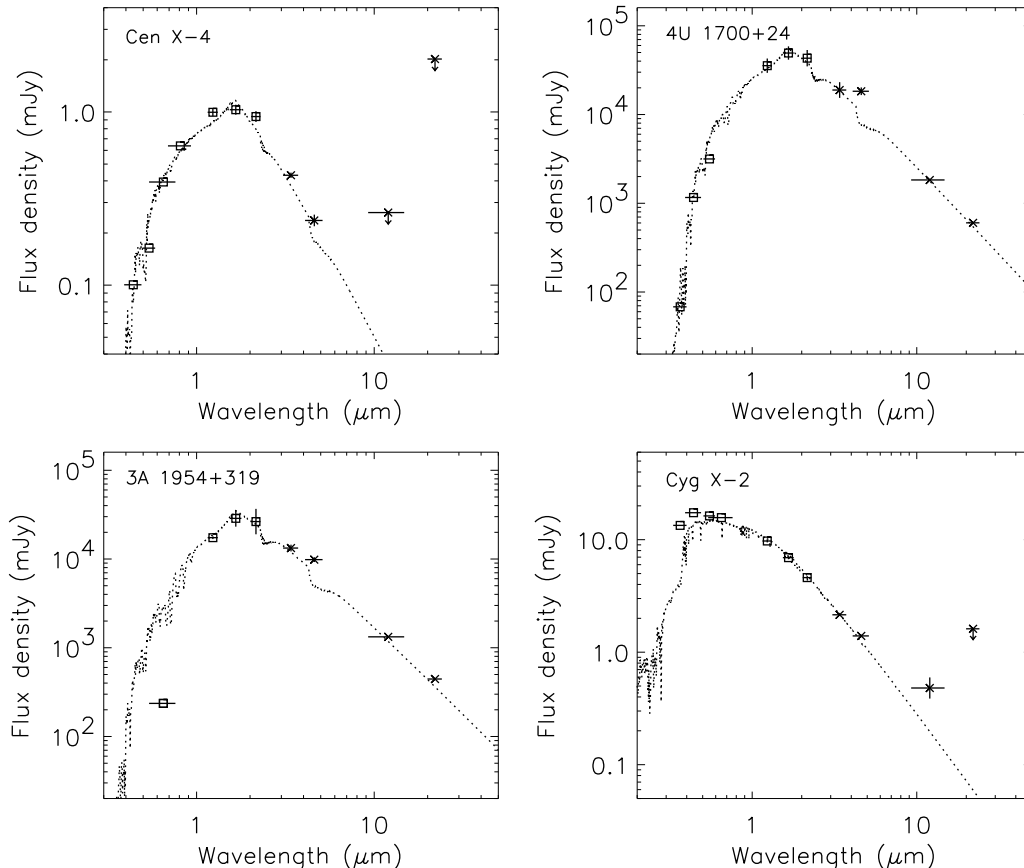


FIG. 2.— Flux density spectra of Cen X-4, 4U 1700+24, 3A 1954+319, and Cyg X-2. The squares are the optical/near-IR data points and crosses are the WISE data points. The dotted curves represent emission from the companion stars.

tected by WISE, with no excess emission found at the WISE bands. The broad-band spectra are shown in Figure 2. Among them, the W2 fluxes of 4U 1700+24 and 3A 1954+319 deviate from the stellar model spectra significantly. However this is due to saturation of the two sources in the WISE W1 and W2 images. They were very bright (~ 3 mag; Table 1), and although large flux uncertainties at the two bands (see Table 1) reflects photometry of the saturated sources, the broad-band spectra indicate that their W2 fluxes were likely overestimated by WISE photometry.

For 3A 1954+319, the companion star was classified as a M4-5III giant from optical spectroscopy by Masetti et al. (2006). Using the R -band magnitude given in the USNO-B1.0 catalogue (Monet et al. 2003) and $V - R = 1.58$ for an M4III star, Masetti et al. (2006) derived $V = 10.7$ and thus estimated a source distance of ~ 1.7 kpc. We checked the USNO-B1.0 catalogue and found that the only measurement for the source is $R = 10.2$, which is not consistent with the value given in Masetti et al. (2006). As can be seen in Figure 2, the R -band flux is an order of magnitude lower than the model spectrum, which may be due to large uncertainties in photometric measurements in the USNO-B1.0 catalogue. The extinction towards this high Galactic latitude ($Gb = 64^\circ$) source is estimated to be very low ($E(B - V) \simeq 0.03$; Schlegel et al. 1998), hard to explain the discrepancy. In any case, from matching an M4 giant

model spectrum to the near-IR 2MASS and WISE data, we found that the ratio of the stellar radius R to distance d is $R/d \simeq 2.7 \times 10^{-9}$, and estimated $d \sim 0.67$ kpc when $R = 80 R_\odot$.

For Cyg X-2, a spectral type of A9 for the companion was identified by Casares et al. (1998). We used a model spectrum of such a giant star to fit the broad-band spectrum, and the model describes the observed IR data points well. Since Cyg X-2 is a bright, persistent X-ray source, in which an accretion disk exists, the optical fluxes contain emission from the disk and thus are above the model spectrum. The W3 flux is above the model spectrum, but we note that the measured magnitude, 11.95, is close to the limiting magnitude of WISE at the W3 band (Wright et al. 2010) and the deviation is likely due to the large uncertainties in the flux measurements of very faint sources. The R/d ratio we obtained was 2.5×10^{-11} . Using the masses of 1.71 and 0.58 M_\odot for the neutron star and companion (Casares et al. 2010), respectively, the Roche lobe radius of the companion is approximately $7.3 R_\odot$, which implies a source distance of 6.7 kpc. This distance value is consistent with 7.2 ± 1.1 kpc, previously estimated by Orosz & Kuulkers (1999).

3.4. Peculiar systems

Two well known systems, Sco X-1 and Her X-1, were detected by the WISE survey. These two neutron star

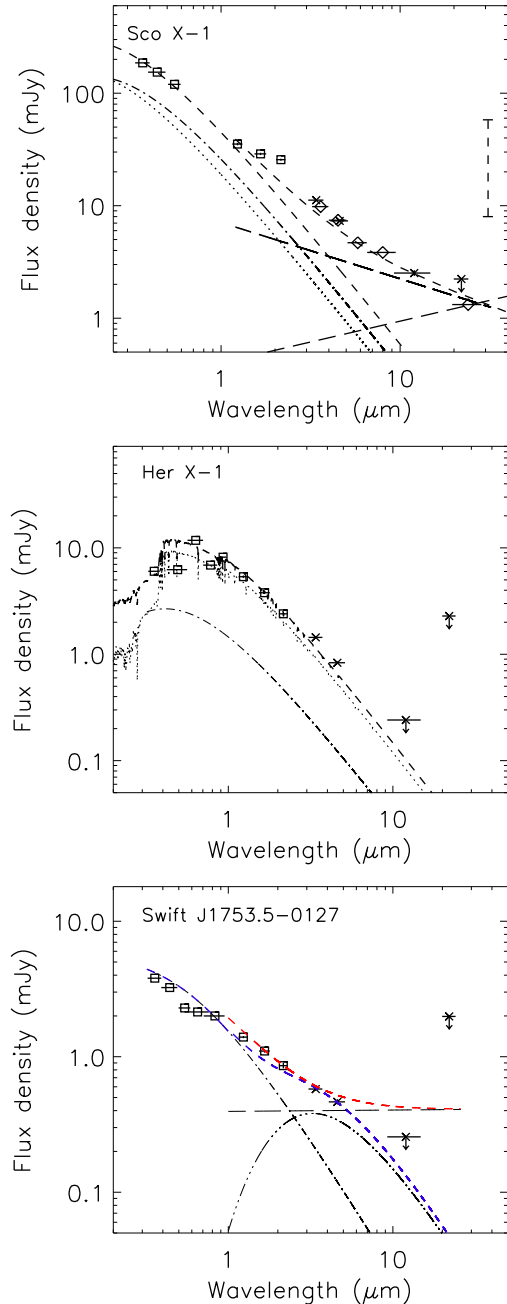


FIG. 3.— Flux density spectra of Sco X-1, Her X-1, and Swift J1753.5–0127. The squares and diamonds are optical/near-IR and *Spitzer* data points, respectively, and crosses are WISE data points. The dotted curves and dash-dotted curves represent emission from the companions and accretion disks, respectively, and the dashed curves represent the total emission from all the components. For Sco X-1 and Swift J1753.5–0127, two other components, the dash-triple-dotted and long dashed curves are discussed (see Section 3.4). The red and blue dashed curves shown for the latter source are the total emission from a power-law and a thermal component, respectively. The large error bar in the top (Sco X-1) panel indicates the range of the obtained radio fluxes in Pandey et al. (2007).

LMXBs are very bright X-ray sources and highly variable, due to accretion activity and orbital modulation. Simultaneous, multiwavelength measurements are particularly required for these two sources in order to conduct data analysis and to determine the presence of excess IR emission and the origin if the excesses are found. In

Figure 3, their broad-band spectra, which are not simultaneous data, are shown.

For Sco X-1, its companion star likely has a mass of $0.42 M_{\odot}$ when a $1.4 M_{\odot}$ neutron star is assumed ($i \simeq 38^{\circ}$; Steeghs & Casares 2002), and probably has a spectral type of earlier than G5 (Bandyopadhyay et al. 1999). At a distance of 2.8 kpc (Bradshaw et al. 1999), such a star has little contribution to the optical fluxes of the source. However given the large X-ray luminosity ($L_X \simeq 2 \times 10^{38} \text{ erg s}^{-1}$; e.g., Bradshaw et al. 2003), we may estimate the irradiated temperature for the companion and it would be of the order of 25,000–30,000 K, depending on the albedo of the companion star. The model spectrum of this strongly irradiated star and that of an irradiated accretion disk (Vrtilek et al. 1990) are shown in Figure 3. The addition of the two spectra is able to describe the optical and near-IR *J*-band data but significantly deviates from the WISE and *Spitzer* data points (the latter are from Revnivtsev et al. 2012), suggesting the need of an additional component. Given that Sco X-1 is known to have a radio jet (e.g., Fomalont et al. 2001), we tested to add a power-law component to eliminate the deviation, and found that $F_{\nu} \sim \nu^{0.5}$ could provide an acceptable fit. However, the power-law component does not connect directly to the radio emission from Sco X-1, which was found to be, for example, in a range of 8–59 mJy at 1.28 GHz (Pandey et al. 2007). A rising, $F_{\nu} \sim \nu^{-0.4}$ spectrum would be needed in order to connect the *Spitzer* 24 μm datum to the radio data. We realized that since the data points shown in Figure 3 were not simultaneously obtained, an alternative explanation for the discrepancy is that during either the WISE or *Spitzer* observations, whose flux measurements are consistent with each other, the radio emission would have been much faint if the IR emission had arisen from the jet.

For Her X-1, by studying its ultraviolet spectra, Cheng et al. (1995) found that a model that contains a companion of late A spectral type plus an X-ray irradiated disk could provide a good fit. Here we used the binary parameters estimated by Reynolds et al. (1997), the masses of $1.5 M_{\odot}$ and $2.3 M_{\odot}$ for the neutron star and companion, respectively, and found that the broad-band data basically could be described by the model emission. Probably because our data were not simultaneous and the contribution from the companion was underestimated (emission from a late type A star with a Roche-lobe radius of $3.85 R_{\odot}$ was used), the distance had to be 5.8 kpc, lower than 6.6 ± 0.4 kpc estimated by Reynolds et al. (1997). In any case our analysis shows that the IR data points are consistent with being a Rayleigh-Jeans tail of thermal emission and no excess emission was found at the IR bands.

The black hole candidate Swift J1753.5–0127 was discovered in 2005 (Palmer et al. 2005). Since then, many studies of the binary have been carried out (e.g., Froning et al. 2014 and references therein). In Figure 3, the broad-band optical and near-IR data from Froning et al. (2014) are shown, which were obtained in 2012 nearly simultaneously. The model fit, produced from a thin, steady-state accretion disk, is also from Froning et al. (2014), and can generally describe the source’s emission in the range of from ultraviolet to near-

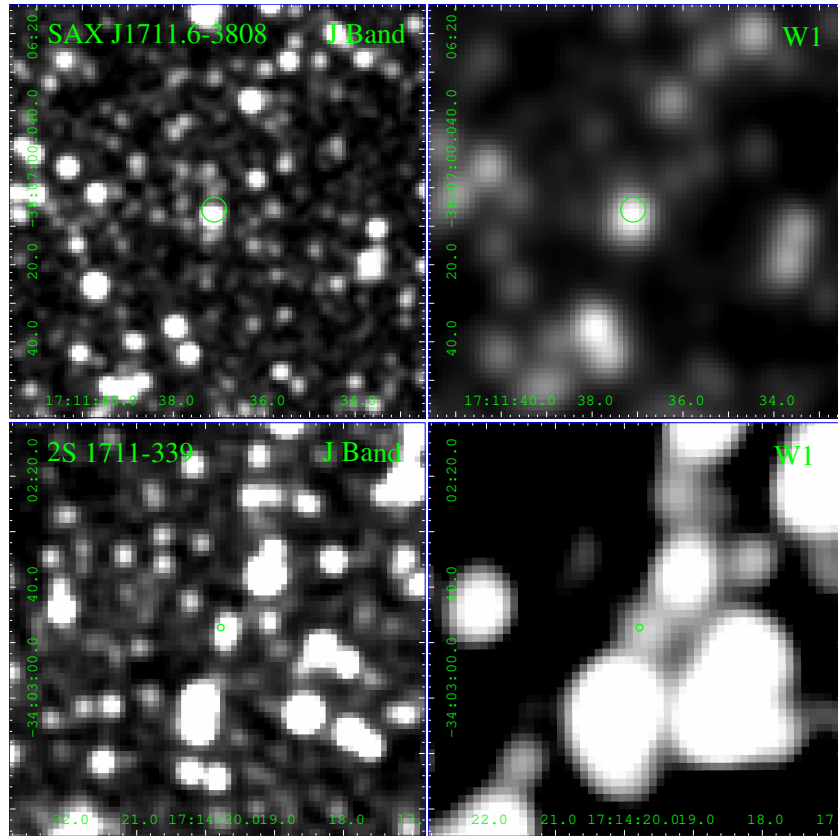


FIG. 4.— Near-IR J band (left panels) and WISE W1 band (right panels) images of the fields of SAX J1711.6–3808 and 2S 1711–339. The X-ray positions are indicated by the circles in the centers of the images.

IR wavelengths. The deviation starts from near-IR H band, which was noted by Froning et al. (2014), and it is so significant at the WISE bands that an additional component is clearly needed. The binary is known to have a jet (Soleri et al. 2010). The radio observation that was closest to the WISE observations was carried out in 2009 June, which found a flux of 0.4 mJy at 8.4 GHz (Soleri et al. 2010). A power-law spectrum $F_\nu \sim \nu^{-0.01}$, presumably from the jet and connects to the radio datum, can explain the IR excesses, but is not allowed by the WISE W3 band flux upper limit. Again like the Sco X-1 case, in order to connect to the radio data, a rising spectrum from mid-IR (at the wavelength of $\sim 12 \mu\text{m}$) is needed. Alternatively, a circumbinary debris disk may also explain the IR excesses. However, since the companion star was not seen in the emission from the binary, no constraints on the disk temperature can be set. To produce the IR spectrum of the disk shown in Figure 3, the temperature at $1.7a$ was 2500 K, too high to be the inner edge of a dust disk. A slightly larger inner disk radius is needed. In addition the outer radius was $5.6a$, larger than that in the A0620–00 and XTE J1118+480 cases.

3.5. Candidate counterparts

Little information is available for the two remaining sources: SAX J1711.6–3808 and 2S 1711–339. The 2MASS J band and WISE W1 band images for each of them are shown in Figure 4. Given that the WISE candidate counterparts were detected by 2MASS, we further compared their 2MASS positions with the reported X-ray positions, since the 2MASS positions have a systematic

uncertainty of only $0''.15$, much more accurate than that of the WISE. For SAX J1711.6–3808, the X-ray positional uncertainty is $3''.2$, and from the 2MASS J -band image, it can be seen that it is located in a crowded field, indicating that the chance of coincidence is high. For 2S 1711–339, the *Chandra* position with an uncertainty of $0''.6$ was reported (Wilson et al. 2003; Torres et al. 2004). The separation distance of the 2MASS source to the position is $1''.2$, approximately 2σ away. Given these, we only suggest the WISE sources as the candidate counterparts.

4. DISCUSSION

Searching through WISE data, we have found 13 counterparts and 2 candidate counterparts among 187 LMXBs catalogued in Liu et al. (2007). By collecting published results and/or analyzing the constructed broad-band spectra for the 13 counterparts, we have identified the origin of the WISE-detected emission. Four of them probably have a candidate circumbinary disk, two harbor a jet, four had thermal emission from their companion stars, and three are peculiar systems with the origin of their IR emission more or less uncertain. It should be noted that these LMXBs are highly variable sources, due to accretion and/or related activities. For the two jet systems, simultaneous multiwavelength observations have been well carried out (e.g., Migliari et al. 2010), but for the other systems the broad-band data used and analyzed in this work are from different epochs, and therefore our studies of the LMXBs are qualitative at most. In order to quantitatively constrain the properties of the candidate circumbinary disk systems or to identify the origin of the IR emission detected from the three pe-

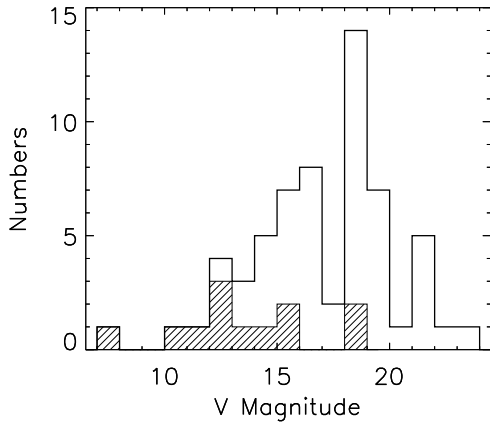


FIG. 5.— V magnitude distribution of 61 LMXBs that have reported V measurements. The filled histogram marks that of the 12 LMXBs with the WISE counterparts. GRS 1915+105 is not included due to high extinction.

cular systems, simultaneous observations at from X-ray, optical/IR, to radio frequencies should be carried out.

For the candidate circumbinary disk systems, Gallo et al. (2007) have proposed the jet scenario to explain the excess IR emission seen in A0620–00 and XTE J1118+480. Given the ubiquity of the presence of jets in the LMXBs (Fender 2006), the jet scenario is also plausible. Detection of dust signatures such as the PAH emission features seen in GRS 1915+105 is needed in order to verify the presence of a dust disk. On the other hand, the case of GRS 1915+105, a well-known microquasar, has shown that an LMXB can harbor both a circumbinary disk and a jet. Thus the two binaries could also have the both. For GX 1+4, although we can not determine if the excess emission arises from a dust shell or a circumbinary disk, the WISE detection of the excesses has revealed another interesting aspect for this binary: the giant-star companion’s significant mass loss is also observable at IR wavelengths.

Finally it is interesting to check the detectability of the LMXBs by an IR survey like WISE. In Figure 5, we show the numbers of the LMXBs as the function of their V magnitude reported in Liu et al. (2007). There are totally 61 LMXBs that have a reported V magnitude value. The distribution of the 12 LMXBs with the WISE counterparts, not including GRS 1915+105 due to extremely high extinction, is shown as the filled histogram. It is not surprising that the WISE-detected sources are among the brightest. The two exceptions are at 18–19 mag, which are 4U 0614+091 and GX 1+4, the first due to the rising spectrum of its jet (Migliari et al. 2006) and the latter due to high extinction (Table 2). From the statistics based on this small sample, while the bias towards the intrinsically bright X-ray sources (such as Sco X-1 and Her X-1) exists, we may suspect that more than half of the LMXBs would have non-stellar IR emission, due to the presence of a jet, a circumbinary debris disk, or the both.

We thank Fuguo Xie for helpful discussion about jet systems among the X-ray binaries. The publication makes use of data products from the Wide-field Infrared Survey Explorer, which is a joint project of the University of California, Los Angeles, and the Jet Propulsion Laboratory/California Institute of Technology, funded by NASA. This publication also makes use of data products from the Two Micron All Sky Survey, which is a joint project of the University of Massachusetts and the Infrared Processing and Analysis Center/California Institute of Technology, funded by the National Aeronautics and Space Administration and the National Science Foundation.

This research was supported by the National Natural Science Foundation of China (11373055) and the Strategic Priority Research Program “The Emergence of Cosmological Structures” of the Chinese Academy of Sciences (Grant No. XDB09000000). Z.W. is a Research Fellow of the One-Hundred-Talents project of Chinese Academy of Sciences.

REFERENCES

- Abazajian, K. N., et al. 2009, *ApJS*, 182, 543
- Bandyopadhyay, R. M., Shahbaz, T., Charles, P. A., & Naylor, T. 1999, *MNRAS*, 306, 417
- Blair, W. P., Raymond, J. C., Dupree, A. K., Wu, C.-C., Holm, A. V., & Swank, J. H. 1984, *ApJ*, 278, 270
- Boer, M., Greiner, J., & Motch, C. 1996, *A&A*, 305, 835
- Borison, B., Blair, W. P., Davidsen, A. F., Vrtilek, S. D., Raymond, J., Long, K. S., & McCray, R. 1997, *ApJ*, 491, 903
- Bradshaw, C. F., Fomalont, E. B., & Geldzahler, B. J. 1999, *ApJ*, 512, L121
- Bradshaw, C. F., Geldzahler, B. J., & Fomalont, E. B. 2003, *ApJ*, 592, 486
- Buxton, M., & Vennes, S. 2003, *MNRAS*, 342, 105
- Cadotte Bel, M., et al. 2007, *ApJ*, 659, 549
- Casares, J., Charles, P. A., & Kuulkers, E. 1998, *ApJ*, 493, L39
- Casares, J., González Hernández, J. I., Israelian, G., & Rebolo, R. 2010, *MNRAS*, 401, 2517
- Chakrabarty, D., & Roche, P. 1997, *ApJ*, 489, 254
- Chapuis, C., & Corbel, S. 2004, *A&A*, 414, 659
- Cheng, F. H., Vrtilek, S. D., & Raymond, J. C. 1995, *ApJ*, 452, 825
- Chevalier, C., Ilovaisky, S. A., van Paradijs, J., Pedersen, H., & van der Klis, M. 1989, *A&A*, 210, 114
- Chevalier, R. A. 1989, *ApJ*, 346, 847
- Corbel, S., & Fender, R. P. 2002, *ApJ*, 573, L35
- Cowley, A. P., Crampton, D., & Hutchings, J. B. 1979, *ApJ*, 231, 539
- Davidson, A., Malina, R., & Bowyer, S. 1977, *ApJ*, 211, 866
- Davidson, A., Malina, R., Smith, H., Spinrad, H., Margon, B., Mason, K., Hawkins, F., & Sanford, P. 1974, *ApJ*, 193, L25
- Debes, J. H., Hoard, D. W., Wachter, S., Leisawitz, D. T., & Cohen, M. 2011, *ApJS*, 197, 38
- Fender, R. 2006, *Jets from X-ray binaries*, ed. W. H. G. Lewin & M. van der Klis, 381–419
- Fender, R., & Belloni, T. 2004, *ARA&A*, 42, 317
- Fomalont, E. B., Geldzahler, B. J., & Bradshaw, C. F. 2001, *ApJ*, 558, 283
- Forman, W., Jones, C., Cominsky, L., Julien, P., Murray, S., Peters, G., Tananbaum, H., & Giacconi, R. 1978, *ApJS*, 38, 357
- Frank, J., King, A., & Raine, D. J. 2002, *Accretion Power in Astrophysics: Third Edition*
- Froning, C. S., Maccarone, T. J., France, K., Winter, L., Robinson, E. L., Hynes, R. I., & Lewis, F. 2014, *ApJ*, 780, 48
- Gallo, E. 2010, in *Lecture Notes in Physics*, Berlin Springer Verlag, Vol. 794, Lecture Notes in Physics, Berlin Springer Verlag, ed. T. Belloni, 85
- Gallo, E., Migliari, S., Markoff, S., Tomsick, J. A., Bailyn, C. D., Berta, S., Fender, R., & Miller-Jones, J. C. A. 2007, *ApJ*, 670, 600

- Galloway, D. K., Sokoloski, J. L., & Kenyon, S. J. 2002, *ApJ*, 580, 1065
- Gandhi, P., et al. 2011, *ApJ*, 740, L13
- Garcia, M., et al. 1983, *ApJ*, 267, 291
- Gelino, D. M., Balman, Ş., Kızıloğlu, Ü., Yılmaz, A., Kalemci, E., & Tomsick, J. A. 2006, *ApJ*, 642, 438
- Gelino, D. M., Harrison, T. E., & Orosz, J. A. 2001, *AJ*, 122, 2668
- Gottlieb, E. W., Wright, E. L., & Liller, W. 1975, *ApJ*, 195, L33
- Greiner, J., Cuby, J. G., & McCaughrean, M. J. 2001, *Nature*, 414, 522
- Hinkle, K. H., Fekel, F. C., Joyce, R. R., Wood, P. R., Smith, V. V., & Lebzelter, T. 2006, *ApJ*, 641, 479
- Hynes, R. I., Mauche, C. W., Haswell, C. A., Shrader, C. R., Cui, W., & Chaty, S. 2000, *ApJ*, 539, L37
- Hynes, R. I., Steeghs, D., Casares, J., Charles, P. A., & O'Brien, K. 2003, *ApJ*, 583, L95
- Indebetouw, R., et al. 2005, *ApJ*, 619, 931
- in't Zand, J. J. M., et al. 2002, *A&A*, 389, L43
- Kong, A. K. H., Kuulkers, E., Charles, P. A., & Homer, L. 2000, *MNRAS*, 312, L49
- Kurucz, R. L. 1993, *VizieR Online Data Catalog*, 6039, 0
- Liu, Q. Z., van Paradijs, J., & van den Heuvel, E. P. J. 2007, *A&A*, 469, 807
- Masetti, N., Orlandini, M., Palazzi, E., Amati, L., & Frontera, F. 2006, *A&A*, 453, 295
- Masetti, N., et al. 2002, *A&A*, 382, 104
- McClintock, J. E., Garcia, M. R., Caldwell, N., Falco, E. E., Garnavich, P. M., & Zhao, P. 2001, *ApJ*, 551, L147
- McClintock, J. E., Narayan, R., Garcia, M. R., Orosz, J. A., Remillard, R. A., & Murray, S. S. 2003, *ApJ*, 593, 435
- McClintock, J. E., & Remillard, R. A. 1986, *ApJ*, 308, 110
- McClintock, J. E., Remillard, R. A., Petro, L. D., Hammerschlag-Hensberge, G., & Proffitt, C. R. 1984, *ApJ*, 283, 794
- Migliari, S., Tomsick, J. A., Maccarone, T. J., Gallo, E., Fender, R. P., Nelemans, G., & Russell, D. M. 2006, *ApJ*, 643, L41
- Migliari, S., et al. 2010, *ApJ*, 710, 117
- Monet, D. G., et al. 2003, *AJ*, 125, 984
- Muno, M. P., & Mauerhan, J. 2006, *ApJ*, 648, L135
- Neilsen, J. 2013, *Advances in Space Research*, 52, 732
- Orosz, J. A., & Kuulkers, E. 1999, *MNRAS*, 305, 132
- Paerels, F., et al. 2001, *ApJ*, 546, 338
- Palmer, D. M., Barthelmey, S. D., Cummings, J. R., Gehrels, N., Krimm, H. A., Markwardt, C. B., Sakamoto, T., & Tueller, J. 2005, *The Astronomer's Telegram*, 546, 1
- Pandey, M., Rao, A. P., Ishwara-Chandra, C. H., Durouchoux, P., & Manchanda, R. K. 2007, *A&A*, 463, 567
- Podsiadlowski, P., Rappaport, S., & Pfahl, E. D. 2002, *ApJ*, 565, 1107
- Rahoui, F., Chaty, S., Rodriguez, J., Fuchs, Y., Mirabel, I. F., & Pooley, G. G. 2010, *ApJ*, 715, 1191
- Revnivtsev, M. G., Zolotukhin, I. Y., & Meshcheryakov, A. V. 2012, *MNRAS*, 421, 2846
- Reynolds, A. P., Quaintrell, H., Still, M. D., Roche, P., Chakrabarty, D., & Levine, S. E. 1997, *MNRAS*, 288, 43
- Russell, D. M., Fender, R. P., Hynes, R. I., Brocksopp, C., Homan, J., Jonker, P. G., & Buxton, M. M. 2006, *MNRAS*, 371, 1334
- Russell, D. M., Fender, R. P., & Jonker, P. G. 2007, *MNRAS*, 379, 1108
- Schlegel, D. J., Finkbeiner, D. P., & Davis, M. 1998, *ApJ*, 500, 525
- Shahbaz, T., Naylor, T., & Charles, P. A. 1993, *MNRAS*, 265, 655
- Shakura, N. I., & Sunyaev, R. A. 1973, *A&A*, 24, 337
- Skrutskie, M. F., et al. 2006, *AJ*, 131, 1163
- Soleri, P., Fender, R., Tudose, V., et al. 2010, *MNRAS*, 406, 1471
- Steenhals, D., & Casares, J. 2002, *ApJ*, 568, 273
- Still, M., Roming, P., Brocksopp, C., & Markwardt, C. B. 2005, *The Astronomer's Telegram*, 553, 1
- Taam, R. E., Sandquist, E. L., & Dubus, G. 2003, *ApJ*, 592, 1124
- Tananbaum, H., Gursky, H., Kellogg, E. M., Levinson, R., Schreier, E., & Giacconi, R. 1972, *ApJ*, 174, L143
- Tomsick, J. A., Chaty, S., Rodriguez, J., Walter, R., & Kaaret, P. 2008, *ApJ*, 685, 1143
- Torres, M. A. P., McClintock, J. E., Garcia, M. R., & Murray, S. S. 2004, *The Astronomer's Telegram*, 233, 1
- Uemura, M., et al. 2000, *PASJ*, 52, L15
- van der Veen, W. E. C. J., Waters, L. B. F. M., Trams, N. R., & Matthews, H. E. 1994, *A&A*, 285, 551
- Vrtilek, S. D., Penninx, W., Raymond, J. C., Verbunt, F., Hertz, P., Wood, K., Lewin, W. H. G., & Mitsuda, K. 1991, *ApJ*, 376, 278
- Vrtilek, S. D., Raymond, J. C., Garcia, M. R., Verbunt, F., Hasinger, G., & Kurster, M. 1990, *A&A*, 235, 162
- Waters, L. B. F. M., Cote, J., & Geballe, T. R. 1988, *A&A*, 203, 348
- Weingartner, J. C., & Draine, B. T. 2001, *ApJ*, 548, 296
- Wilson, C. A., Patel, S. K., Kouveliotou, C., Jonker, P. G., van der Klis, M., Lewin, W. H. G., Belloni, T., & Méndez, M. 2003, *ApJ*, 596, 1220
- Wright, E. L., et al. 2010, *AJ*, 140, 1868
- Wu, C.-C., Aalders, J. W. G., van Duinen, R. J., Kester, D., & Wesselius, P. R. 1976, *A&A*, 50, 445
- Yuan, F., Bu, D., & Wu, M. 2012, *ApJ*, 761, 130
- Yuan, F., & Narayan, R. 2014, *ArXiv e-prints*
- Zdziarski, A. A., Gierliński, M., Mikołajewska, J., Wardziński, G., Smith, D. M., Harmon, B. A., & Kitamoto, S. 2004, *MNRAS*, 351, 791
- Zurita, C., et al. 2002, *MNRAS*, 333, 791

TABLE 1
SUMMARY OF WISE MEASUREMENTS OF THE (CANDIDATE) COUNTERPARTS OF 15 LMXBs

Source	δ ($''$)	Obs. date	W1 (mag)	W2 (mag)	W3 ^a (mag)	W4 ^a (mag)	J (mag)	H (mag)	K (mag)
A0620–00	0.88	2010-03-19	14.17±0.03	13.84±0.04	12.71	9.11	15.49±0.05	14.74±0.06	14.38±0.07
4U 0614+091	0.57	2010-03-18	16.02±0.09	15.19±0.14	11.75±0.25	8.78			
XTE J1118+480	0.88	2010-05-10	16.40±0.08	15.85±0.17	12.92	9.24	12.76±0.02	12.44±0.03	12.08±0.02
4U 1456–32 (Cen X-4)	0.65	2010-02-05	14.65±0.04	14.66±0.08	12.62	9.04	15.60±0.06	15.05±0.07	14.66±0.08
H 1617–155 (Sco X-1)	0.25	2010-02-23	11.16±0.02	10.97±0.02	10.20±0.06	8.95	11.91±0.03	11.55±0.03	11.15±0.02
2A 1655+353 (Her X-1)	0.19	2010-02-21	13.32±0.03	13.28±0.03	12.70	8.90	13.73±0.03	13.61±0.03	13.63±0.03
4U 1659–487 (GX 339–4)	1.06	2010-03-10	9.62±0.03	8.77±0.02	6.82±0.02	5.17±0.04	15.91±0.14	15.40±0.15	14.97±0.14
4U 1700+24	0.16	2010-02-27	3.04±0.22	2.43±0.11	3.01±0.03	2.85±0.03	4.17±0.20	3.32±0.19	2.99±0.23
SAX J1711.6–3808	1.81	2010-03-10	8.74±0.02	8.66±0.02	8.35±0.05	7.60±0.18	12.46±0.03	10.43±0.03	9.43±0.03
2S 1711–339	1.19	2010-03-11	12.37±0.04	12.54±0.06	9.13±0.08	8.15±0.32	14.34±0.04	13.19±0.03	12.86±0.04
4U 1724–307	1.38	2010-03-13	7.05±0.02	6.99±0.02	7.46±0.04	6.38±0.09	10.33±0.10	9.09±0.09	8.56±0.07
3A 1728–247 (GX 1+4)	0.19	2010-03-13	7.48±0.03	7.24±0.02	6.77±0.02	6.33±0.06	10.10±0.02	8.70±0.05	7.98±0.02
Swift J1753.5–0127	0.11	2010-03-17	14.31±0.03	13.91±0.05	12.64	9.05			
GRS 1915+105	0.11	2010-04-11	12.11±0.03	11.45±0.04	9.86±0.24	7.68±0.33	15.43	14.37±0.06	12.90±0.06
3A 1954+319	0.98	2010-04-27	3.41±0.10	3.10±0.07	3.35±0.01	3.18±0.02	4.91±0.04	3.88±0.23	3.51±0.36
4U 2142+38 (Cyg X-2)	1.18	2010-06-03	12.89±0.02	12.72±0.03	11.95±0.24	9.28	13.40±0.03	13.16±0.04	13.05±0.03

^a The magnitude values with no uncertainty given are upper limits.

TABLE 2
PROPERTIES OF THE 15 LMXBs

Name	Type	Optical	Spectral Type	P_{orb} (hr)	Distance (kpc)	Optical data	$E(B - V)$ (mag)	References
A0620–00	BH	V616 Mon	K4V	7.75	1.16±0.11	<i>BVRI</i>	0.39	1,2,3
4U 0614+091	NS	V1055 Ori			1.5~3	<i>UBV</i>	0.3	4,5,6
XTE J1118+480	BH	KV UMa	K5V~K7V	4.08	1.8±0.60	<i>R</i>	0.013	7,8,9,10,11
4U 1456–32 (Cen X-4)	NS	V822 Cen	K5V	15.1	1.2±0.3	<i>BVRI</i>	0.1	12,13,14
H 1617–155 (Sco X-1)	NS	V818 Sco		18.9	2.8±0.3	<i>UBV</i>	0.3	15,16,17
2A 1655+353 (Her X-1)	NS	HZ Her		40.8	6.6±0.4	<i>u'g'r'i'z'</i>	0.05	18,19,20,21
4U 1659–487 (GX 339–4)	BH	V821 Ara		42.14	8~2	<i>BV</i>	1.1	22,23,24,25
4U 1700+24		HD 154791	M2III	404d	0.42~0.04	<i>UBV</i>	0.044	26,27,28
SAX J1711.6–3808	BH						5	29
2S 1711–339	NS?					<i>R</i>		30
3A 1728–247 (GX 1+4)	NS	V2116 Oph	M5III	1160.8d	4.3	<i>BVR</i>	1.63	31,32
Swift J1753.5–0127	BH				6	<i>BVRI</i>	0.36	33,34
GRS 1915+105	BH	V1487 Aql		804	9.0±3.0		8.6	35,36,37
3A 1954+319	NS?		M4III~M5III		1.7	<i>V</i>		38
4U 2142+38 (Cyg X-2)	NS	V1341 Cyg	A9III	236.2	7.2±1.1	<i>UBVR</i>	0.40	39,40,41,42

REFERENCES. — (1) McClintock & Remillard (1986); (2) Gelino et al. (2001); (3) Wu et al. (1976); (4) Paerels et al. (2001); (5) Davidsen et al. (1974); (6) Russell et al. (2007); (7) Uemura et al. (2000); (8) McClintock et al. (2001); (9) Zurita et al. (2002); (10) Hynes et al. (2000); (11) McClintock et al. (2003); (12) Chevalier et al. (1989); (13) Shahbaz et al. (1993); (14) Blair et al. (1984); (15) Gottlieb et al. (1975); (16) Bradshaw et al. (1999); (17) Vrtilik et al. (1991); (18) Tananbaum et al. (1972); (19) Reynolds et al. (1997); (20) Abazajian et al. (2009); (21) Boroson et al. (1997); (22) Hynes et al. (2003); (23) Zdziarski et al. (2004); (24) Kong et al. (2000); (25) Buxton & Vennes (2003); (26) Galloway et al. (2002); (27) Masetti et al. (2002); (28) Garcia et al. (1983); (29) in't Zand et al. (2002); (30) Torres et al. (2004); (31) Hinkle et al. (2006); (32) Chakrabarty & Roche (1997); (33) Cadolle Bel et al. (2007); (34) Still et al. (2005); (35) Greiner et al. (2001); (36) Boer et al. (1996); (37) Chapuis & Corbel (2004); (38) Masetti et al. (2006); (39) Cowley et al. (1979); (40) Casares et al. (1998); (41) Orosz & Kuulkers (1999); (42) McClintock et al. (1984);